World Journal of Hepatology

Submit a Manuscript: http://www.wjgnet.com/esps/
Help Desk: http://www.wjgnet.com/esps/helpdesk.aspx
DOI: 10.4254/wjh.v8.i16.673

World J Hepatol 2016 June 8; 8(16): 673-684
ISSN 1948-5182 (online)

ORIGINAL ARTICLE

Basic Study

Obese diet-induced mouse models of nonalcoholic steatohepatitis-tracking disease by liver biopsy

Maria Nicoline Baandrup Kristiansen, Sanne Skovgård Veidal, Kristoffer Tobias Gustav Rigbolt, Kirstine Sloth Tølbøl, Jonathan David Roth, Jacob Jelsing, Niels Vrang, Michael Feigh

Maria Nicoline Baandrup Kristiansen, Sanne Skovgård Veidal, Kristoffer Tobias Gustav Rigbolt, Kirstine Sloth Tølbøl, Jacob Jelsing, Niels Vrang, Michael Feigh, Gubra Aps, 2970 Hørsholm, Denmark

Jonathan David Roth, Intercept Pharmaceuticals, Inc., San Diego, CA 9212, United States

Author contributions: Kristiansen MNB, Veidal SS, Rigbolt KTG, Tølbøl KS and Feigh M performed the experiments and analyzed the data; Rigbolt KTG performed the molecular investigations; Kristiansen MNB and Veidal SS performed the histological analysis; Veidal SS, Rigbolt KTG, Roth JD, Jelsing J, Vrang N and Feigh M designed and coordinated the research; Kristiansen MNB, Veidal SS, Rigbolt KTG, Tølbøl KS, Roth JD, Jelsing J, Vrang N and Feigh M wrote the paper.

Institutional review board statement: This study includes no data or material from patients. We confirm that all of the required permissions for this study were obtained from our local authorities as mentioned in the Institutional animal care and use committee statement.

Institutional animal care and use committee statement: All procedures involving animals were reviewed and approved by the Danish Committee for animal research and covered by a personal license for Jacob Jelsing (2013-15-2934-00784). All of the institutional and national guidelines for the care and use of laboratory animals were followed.

Conflict-of-interest statement: There are no patents, products in development or marked products to declare.

Data sharing statement: No additional data are available.

Correspondence to: Michael Feigh, PhD, Gubra Aps, Hørsholm Kongevej 11B, 2970 Hørsholm, Denmark. mfe@gubra.dk
Telephone: +45-31522651

Received: February 11, 2016
Peer-review started: February 12, 2016
First decision: March 9, 2016
Revised: April 1, 2016
Accepted: April 20, 2016
Article in press: April 22, 2016
Published online: June 8, 2016

Abstract

AIM: To characterize development of diet-induced nonalcoholic steatohepatitis (NASH) by performing liver biopsy in wild-type and genetically obese mice.

METHODS: Male wild-type C57BL/6J (C57) mice (DIO-NASH) and male *Lep*^{ob}/*Lep*^{ob} (*ob*/*ob*) mice (*ob*/*ob*-NASH) were maintained on a diet high in trans-fat (40%), fructose (22%) and cholesterol (2%) for 26 and 12 wk, respectively. A normal chow diet served as control in C57 mice (lean chow) and *ob*/*ob* mice (*ob*/*ob* chow). After the diet-induction period, mice were liver biopsied and a blinded histological assessment of steatosis and fibrosis was conducted. Mice were then stratified into groups counterbalanced for steatosis score and fibrosis stage and continued on diet and to receive daily PO dosing of vehicle for 8 wk. Global gene expression in liver tissue was assessed by RNA sequencing and bioinformatics. Metabolic parameters, plasma liver enzymes and lipids (total cholesterol, triglycerides) as well as hepatic lipids and collagen content were measured by biochemical analysis. Non-alcoholic fatty liver disease activity score (NAS) (steatosis/inflammation/ballooning

degeneration) and fibrosis were scored. Steatosis and fibrosis were also quantified using percent fractional area.

RESULTS: Diet-induction for 26 and 12 wk in DIO-NASH and *ob*/*ob*-NASH mice, respectively, elicited progressive metabolic perturbations characterized by increased adiposity, total cholesterol and elevated plasma liver enzymes. The diet also induced clear histological features of NASH including hepatosteatosis and fibrosis. Overall, the metabolic NASH phenotype was more pronounced in *ob*/*ob*-NASH *vs* DIO-NASH mice. During the eight week repeated vehicle dosing period, the metabolic phenotype was sustained in DIO-NASH and *ob*/*ob*-NASH mice in conjunction with hepatomegaly and increased hepatic lipids and collagen accumulation. Histopathological scoring demonstrated significantly increased NAS of DIO-NASH mice (0 *vs* 4.7 ± 0.4, $P < 0.001$ compared to lean chow) and ob/ob-NASH mice (2.4 ± 0.3 *vs* 6.3 ± 0.2, $P < 0.001$ compared to *ob*/*ob* chow), respectively. Furthermore, fibrosis stage was significantly elevated for DIO-NASH mice (0 *vs* 1.2 ± 0.2, $P < 0.05$ compared to lean chow) and *ob*/*ob* NASH (0.1 ± 0.1 *vs* 3.0 ± 0.2, $P < 0.001$ compared to *ob*/*ob* chow). Notably, fibrosis stage was significantly ($P < 0.001$) increased in *ob*/*ob*-NASH mice, when compared to DIO-NASH mice.

CONCLUSION: These data introduce the obese diet-induced DIO-NASH and *ob*/*ob*-NASH mouse models with biopsy-confirmed individual disease staging as a preclinical platform for evaluation of novel NASH therapeutics.

Key words: Nonalcoholic steatohepatitis; Liver biopsy; Diet-induced obesity; Nonalcoholic fatty liver disease; Fibrosis

Core tip: We characterize the development and progression of diet-induced nonalcoholic steatohepatitis (NASH) in a wild-type and a genetically obese mouse model. We confirm that a diet high in trans-fat, fructose and cholesterol, develops key histological hallmarks of NASH (steatosis, inflammation, ballooning degeneration) in conjunction with fibrosis. Concomitantly, marked alterations in NASH associated gene expression pathways can be evaluated by RNAseq analysis. In addition, we describe that performing a baseline liver biopsy enables individual disease staging for subsequent stratified randomization of animals into study groups. Finally, we show these models' utility for a chronic repeated dosing study to evaluate pharmacological intervention.

Kristiansen MNB, Veidal SS, Rigbolt KTG, Tølbøl KS, Roth JD, Jelsing J, Vrang N, Feigh M. Obese diet-induced mouse models of nonalcoholic steatohepatitis-tracking disease by liver biopsy. *World J Hepatol* 2016; 8(16): 673-684 Available from: URL: http://www.wjgnet.com/1948-5182/full/v8/i16/673.htm DOI: http://dx.doi.org/10.4254/wjh.v8.i16.673

INTRODUCTION

It is generally accepted that along with increasing rates of obesity, type 2 diabetes and metabolic syndrome, the incidence and prevalence of patients with nonalcoholic fatty liver disease (NAFLD) continues to rise[1-4]. NAFLD is considered the hepatic manifestation of the metabolic syndrome and covers a variety of pathologies ranging from simple hepatic steatosis (accumulation of triglycerides in hepatocytes) to nonalcoholic steatohepatitis (NASH), characterized by inflammation, cellular ballooning and fibrosis in varying degrees[1-3]. The pathogenesis of NASH is described by the "two-hit" hypothesis, the first hit being fat accumulation in hepatocytes, while the "second hit", *e.g.,* oxidative stress, apoptosis or mitochondrial dysfunction, causes development of inflammation and fibrosis[5].

There are currently no pharmacological agents specifically approved for the treatment of NASH and disease management is consequently focused on the correction of underlying risk factors (*e.g.,* obesity, insulin resistance and dyslipidemia)[1,6]. A likely contributor to the absence of therapeutics is the paucity of preclinical models resembling human NAFLD/NASH[6]. Historically, several animal models have been developed to represent the pathophysiology, morphological findings, biochemical changes, and clinical features of human NAFLD/NASH. These models are usually divided into two main categories: The diet-induced models and the genetically modified models (transgenic or knockout models)[1]. Some diet-induced models are based on *ad libitum* feeding of diets enriched with various combinations of fat, cholesterol and sugars (*e.g.,* fructose) thereby developing a metabolic phenotype reflected by adiposity and hepatosteatosis, albeit only presenting mild characteristics of NASH and typically lack of liver fibrosis[7,8]. Other dietary models involve feeding nutrient-deficient diets such as the methionine- and choline-deficient diet (MCD). Methionine and choline deficiency impairs liver β-oxidation and the production of very-low density lipoproteins (VLDL) hereby generating a "second hit"[1], eliciting a more severe fibrotic NASH phenotype within hepatic tissue[8,9]. However, these models fail to recapitulate a clinically relevant overall metabolic phenotype as MCD animals demonstrate pronounced weight loss and perturbed energy- and glucose homeostasis[10]. Recently, a novel wild-type diet-induced obese fibrotic NASH mouse model was introduced by Trevaskis *et al*[11], based on the ALIOS diet model[12]. This model, generated by feeding an *ad libitum* diet high in trans-fat, fructose and cholesterol to wild-type C57Bl/6J mice [the Amylin liver NASH model (AMLN)], displayed key hallmarks of clinical NASH[11]. The AMLN mouse model was further optimized by demonstrating a liver biopsy technique for

assessing individual steatosis, inflammation, ballooning degeneration and fibrosis staging, prior to a putative study intervention[6]. Not only does the baseline liver biopsy reduce biological variability by excluding mice that fail to develop NASH prior to initiating therapy, but it also allows for within-subject comparisons over time, thereby increasing statistical power[6].

For the genetically modified NASH models, several studies have implicated a role of individual genes involved in the development of NASH using deletion or overexpression models[7,9]. For example, mice that overexpress the transcription factor sterol regulatory element-binding proteins (SREBPs), a feedback regulatory system controlling intracellular levels of cholesterol and free fatty acids develop a hepatic phenotype resembling NASH. However, like MCD-fed mice, SREBP overexpression does not induce a metabolic profile consistent with obesity and insulin resistance[13]. In contrast, impairment of leptin signaling (*e.g.*, *db*/*db* mice) results in obesity, insulin resistance and diabetes[14]. Leptin-deficient mice (Lep^{ob}/Lep^{ob}) are predisposed to develop steatohepatitis, however, when maintained on regular rodent chow they do not develop fibrosis[11]. In fact, it was previously postulated that Lep^{ob}/Lep^{ob} mice are incapable of developing hepatic fibrosis[9]. This notion was dispelled by the observation that Lep^{ob}/Lep^{ob} mice maintained on the AMLN diet for at least 12 wk do in fact develop the key hallmarks of NASH, including fibrosis[11].

The present study assessed key NASH diagnostic characteristics (*e.g.*, steatosis score, inflammation, ballooning degeneration and fibrosis stage), metabolic endpoints and gene expression signatures in wild-type C57Bl/6J and Lep^{ob}/Lep^{ob} mice, fed the AMLN diet for a total of 34 and 20 wk, respectively, including an eight-week repeated vehicle dosing period. In addition, we demonstrate how a baseline liver biopsy allows for individual disease staging and for stratified randomization into experimental groups with reduced biological variability and for a clear cut analysis of individual response to pharmacological intervention.

MATERIALS AND METHODS

Animals and experimental set-up

All animal experiments were conformed to international accepted principles for the care and use of laboratory animals and were covered by a personal license for Jacob Jelsing (2013-15-2934-00784) issued by the Danish Committee for animal research.

Male C57Bl/6J (C57) and Lep^{ob}/Lep^{ob} (*ob*/*ob*) mice at 5 wk of age were obtained from JanVier (JanVier labs, France), and group housed 5 animals pr. cage under a 12/12 h dark-light cycle. Room temperature was controlled to 22 ℃ ± 1 ℃, with 50% ± 10% humidity. Animals had *ad libitum* access to diet high in fat (40%, of these 18% trans-fat), 40% carbohydrates (20% fructose) and 2% cholesterol (D09100301, Research Diet, United States) previously described as the AMLN diet[6], or regular rodent chow (Altromin 1324, Brogaarden, Denmark), and tap water. Both strains had *ad libitum* access to either the AMLN diet (DIO-NASH, n = 110; *ob*/*ob* NASH, n = 40) or chow (lean chow, n = 10; *ob*/*ob* chow, n = 10). After 26 (DIO-NASH) or 12 wk (*ob*/*ob*-NASH) a liver biopsy was performed for histological assessment of individual fibrosis and steatosis staging at baseline. Following biopsy procedure animals were single housed. An 8-wk vehicle intervention period was conducted in a representative subset of DIO-NASH and *ob*/*ob*-NASH mice, and their respective chow controls. Vehicle dosing consisted of once daily per oral dose of carboxymethyl cellulose (C57 and *ob*/*ob*) and subcutaneous injection with PBS (C57). The rationale was to mimic repeated dosing administration and animal handling in combination with AMLN diet-maintenance. After a total of 34 and 20 wk on AMLN diet for DIO-NASH and *ob*/*ob*-NASH mice, respectively, animals were euthanized and liver tissue collected for histological and biochemical analysis. Total animal numbers for each experiment is indicated in the figures and table.

Baseline liver biopsy after diet-induction

Mice were pretreated with enrofloxazin (Bayer, Germany) (5 mg/mL-1 mL/kg) one day before being biopsied. Prior to biopsy, mice were anesthetized with isoflurane (2%-3%) in 100% oxygen. A small abdominal incision in the midline was made and the left lateral lobe of the liver was exposed. A cone shaped wedge of liver tissue (50-100 mg) was excised from the distal portion of the lobe fixed in 4% paraformaldehyde for histology. The biopsy procedure previously described by Clapper *et al*[6] 2013 was refined using electrocoagulation of the cut surface of the liver by means of bipolar coagulation using ERBE VIO 100C electrosurgical unit (ERBE, United States). The liver was returned to the abdominal cavity, abdominal wall was sutured and skin stapled. Carprofen (Pfizer, United States) (5 mg/mL-0.01 mL/10 g) and enrofloxazin (5 mg/mL-1 mL/kg) were administered intraperitoneal at the time of surgery and at post-operation day one and two, to control postoperative pain relief and infection, respectively.

Hepatic gene expression changes

Gene expression changes were measured in a representative subset of DIO-NASH mice and *ob*/*ob*-NASH. Liver tissue was harvested from the left lateral lobe and snap frozen in liquid nitrogen. Tissue sections (about 50 mg) were homogenized in lysis buffer containing protease inhibitors and used for RNA extraction using NucleoSpin Plus RNA columns (Macherey-Nagel). The quantity of the RNA was analyzed using a Nano Drop 2000 spectrophotometer (Thermo Scientific, United States). RNAseq libraries were prepared with the KAPA poly-A kit (Kapa Biosystems, United States) and sequenced on the NextSeq 500 (Illumina, United States) (single-end, 75 bp reads). Reads were aligned to the GRCm38 Ensembl Mus musculus genome using STAR v.2.4.0[15] and feature counts were obtained using HTseq v.0.6.1[16], both with default parameters. Differential

expression analysis was performed with edgeR[17] and genes with a $P \leqslant 0.05$ after correction for multiple testing using the Benjamini and Hochberg method was regarded as significantly regulated. Pathway analysis of WikiPathways[18] was performed using the statistics module in PathVisio[19].

Body weight and body composition analysis

Body weight was intermittently monitored during the diet-induction period and once daily during the intervention period. Whole-body fat mass was analyzed at baseline (week -1) and week 8 of the intervention period by non-invasive EchoMRI scanning using Echo-MRI-900 (EchoMRI, United States). During the scanning procedure the mice were placed in a restrainer for 90-120 s.

Plasma biochemistry analysis

After diet-induction, a baseline blood sample was collected from the submandibular vein in non-fasted conscious animals and blood sampling was repeated following the intervention period. Plasma levels of alanine aminotransferase (ALT), aspartate aminotransferase (AST), triglycerides (TG) and total cholesterol (TC) were measured using the auto analyzer Cobas C-111 (Roche Diagnostics, Germany). Plasma levels of insulin were measured in duplicates using an AlphaLisa kit (Perkin Elmer), according to the manufacturer's instructions.

Oral glucose tolerance test

An oral glucose tolerance test (OGTT) was performed in week 4 of the intervention period. Animals were fasted for 4 h prior to OGTT. At $t = 0$ an oral glucose load [2 g/kg glucose 200 mg/mL, (Fresenius Kabi, Sweden)] was administered *via* a gastrically placed tube. Blood samples for measuring blood glucose (BG) were collected from the tail vein at $t = 0$, 15, 30, 60 and 120 min. Glucose area under the curve (AUC) calculations were determined as total AUC from the sampling period of 0 to 120 min.

Whole blood glucose analysis

Blood samples for BG analysis were collected into 10 μL heparinized glass capillary tubes and immediately suspended in buffer [0.5 mL of glucose/lactate system solution (EKF-diagnostics, Germany)] and analyzed for glucose using a BIOSEN c-Line glucose meter (EKF-diagnostics, Germany) according to the manufacturer's instructions.

Terminal hepatic hydroxyproline content

Formalin fixed (50 mg) liver tissue was homogenized in 500 μL water. Five hundred microliter concentrated HCl was added to the samples and hydrolyzed at 120 ℃ for three hours. Supernatants were transferred to a 96 well plate and wells were allowed to evaporate dry overnight. Total collagen content in the liver was measured by colorimetric determination of hydroxyproline residues by acid hydrolysis of collagen (Cat no. MAK008, Sigma Aldrich).

Terminal hepatic triglyceride and total cholesterol content

A liver piece (about 100 mg) was collected in FastPrep tubes and snap-frozen in liquid nitrogen. One milliliter 5%NH-40/ddH_2O solution (ab142227, Abcam) was added to the FastPrep tube. The tubes were homogenized in a FastPrep homogenizer and shaken for 2 × 60 s. After homogenization the samples were slowly heated to 80 ℃-100 ℃ in a heating block for three minutes. Samples were allowed to return to room temperature prior to a second round of heating. Next, samples were centrifuged for two minutes at top speed using a microcentrifuge to remove any insoluble material. TG and TC content in liver homogenates are measured in single determinations using auto analyzer Cobas C-111 with commercial kit (Roche Diagnostics, Germany) according to manufacturer's instructions.

Histology assessment and digital image analysis

Baseline liver biopsy and terminal samples were collected from the left lateral lobe (about 100 mg) and fixed overnight in 4% paraformaldehyde. Liver tissue was paraffin embedded and sectioned (3 μm thickness). To assess hepatic morphology and fibrosis, sections were stained with Hematoxylin and Eosin and Sirius Red, respectively, followed by analysis with Visiomorph software (Visiopharm, Denmark). Histological assessment and scoring was performed by a pathologist blinded to the study. NAFLD activity score (NAS) (steatosis/inflammation/ballooning degeneration) and fibrosis stage were performed using the clinical criteria outlined by Kleiner *et al*[20].

Statistical analysis

All data were analyzed using GraphPad Prism 5.0. The results are presented as mean ± standard error of the mean. Statistical significance was evaluated using One-way analysis of variance with Turkey's multiple comparison test, and for histological analysis using Kruskal-Wallis test with Dunn's multiple comparison test. $P < 0.05$ was considered statistical significant.

RESULTS

Male C57 and ob/ob mice developed adiposity and elevated plasma metabolic parameters after AMLN diet-induction

The overall study design is outlined in Figure 1A. Following a diet-induction period of 26 wk, C57 (DIO-NASH) mice demonstrated increased body weight (adiposity), when compared to lean chow animals. In the already obese *ob*/*ob* strain there was no additional effect on body weight noted in *ob*/*ob*-NASH mice relative to chow controls. Whereas all mice experienced slight weight loss following the biopsy, they returned

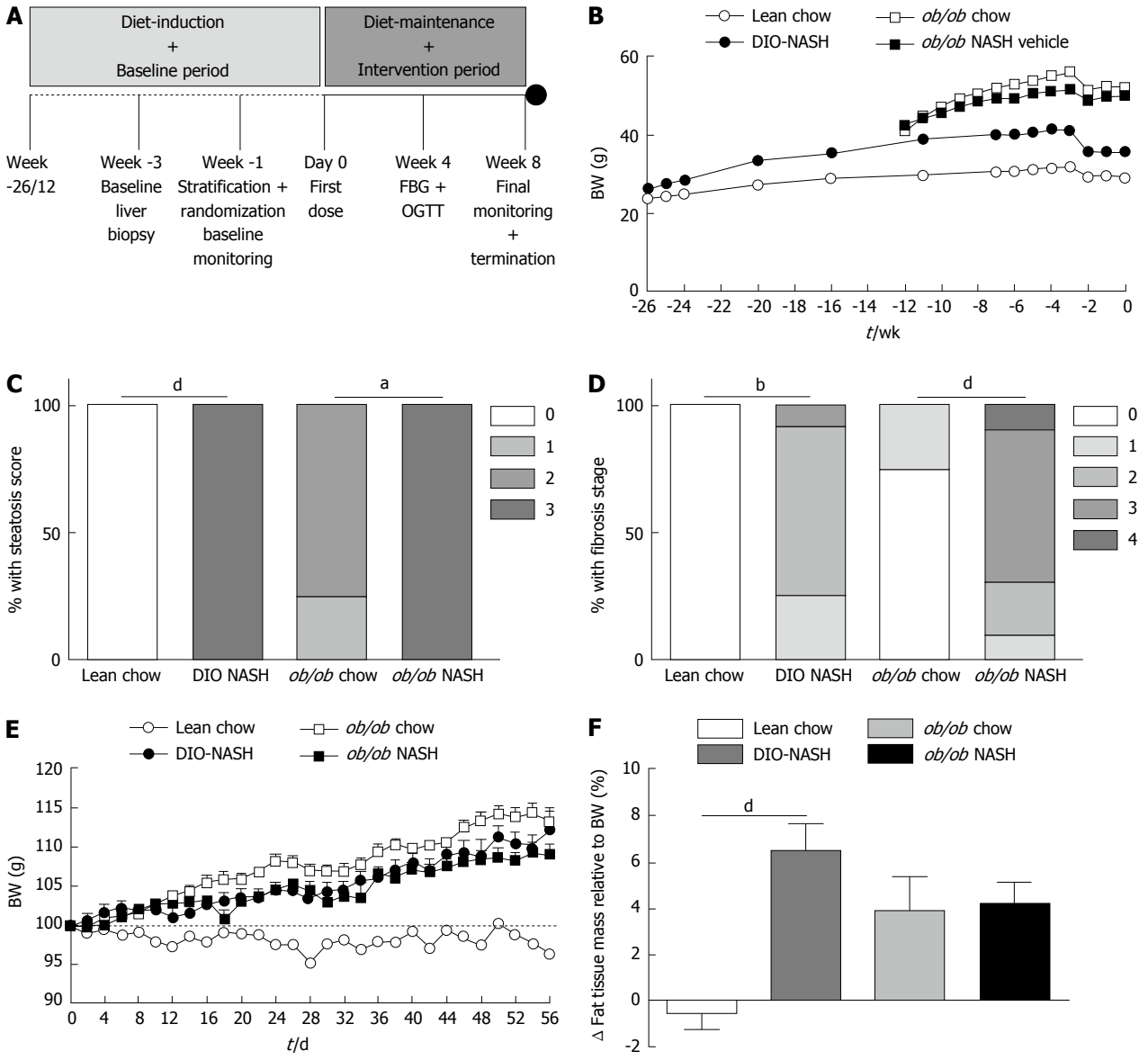

Figure 1 Study design, body weight regulation and liver biopsy-confirmed disease development. A: Study design of the DIO-NASH and *ob/ob* NASH mouse models; B: BW during diet-induction and baseline period (monitoring and biopsy-recovery); C and D: Liver biopsy-derived histopathological assessment of (C) steatosis score (0-3), and (D) fibrosis stage (0-4); E and F: Change in BW (E), and change in adiposity (F), during diet-maintenance and intervention period (repeated vehicle dosing). $^{a}P < 0.05$, $^{b}P < 0.01$, $^{d}P < 0.001$. The results are presented as mean ± SEM. Lean chow (n = 9), DIO-NASH (n = 12), *ob/ob* chow (n = 8), *ob/ob* NASH (n = 10). NASH: Nonalcoholic steatohepatitis; BW: Body weight; OGTT: Oral glucose tolerance test; FBG: Fed blood glucose; SEM: Standard error of the mean.

to a weight stable state within one week (Figure 1B). After diet-induction, DIO-NASH and *ob*/*ob*-NASH mice demonstrated a metabolic NAFLD phenotype, as reflected by elevated levels of plasma total cholesterol (TC) and liver enzymes ALT and AST, when compared to respective chow fed animals. Overall, the *ob*/*ob*-NASH mice demonstrated an accelerated and more pronounced metabolic phenotype, when compared to DIO-NASH mice (Table 1).

Male C57 and ob/ob mice demonstrated biopsy-proven hepatic steatosis and fibrosis after AMLN diet-induction

Histological assessments of biopsied liver tissue revealed that lean chow animals did not develop hepatic steatosis or fibrosis over the 26-wk diet-induction (Figure 1C and D). In contrast, DIO-NASH mice presented with high levels of steatosis (score 3) (Figure 1C) and fibrosis stage ranging from 1-3 (Figure 1D). The *ob*/*ob* chow phenotype displayed mild steatosis (score 1-2) and lack of or only mild fibrosis (stage 1) whereas all ob/ob-NASH mice displayed a steatosis score of 3 (Figure 1C) and a fibrosis stage ranging from 1-4 (Figure 1D).

Altered hepatic gene expression in male C57 and ob/ob mice after AMLN diet-induction

To characterize the effect of 26 wk diet-induction on global liver gene expression, the transcriptome of lean chow *vs* DIO-NASH mice were analyzed by RNAseq[21]. Principal component analysis identified a clear separation between the two groups along the first component,

Table 1 Effect of Amylin liver nonalcoholic steatohepatitis model diet on metabolic parameters, non-alcoholic fatty liver disease activity score/fibrosis stage, body weight/composition and liver weight

	Lean chow *n* = 9	DIO-NASH *n* = 12	*ob/ob* chow *n* = 8	*ob/ob* NASH *n* = 10
Baseline plasma ALT (U/L)	30.7 ± 0.8	133.6 ± 16.3	207.0 ± 58.7	577.4 ± 43.4[d,f]
Terminal plasma ALT (U/L)	31.5 ± 2.9	126.1 ± 19.8	249.7 ± 47.4	670.0 ± 59.0[d,f]
Baseline plasma AST (U/L)	46.5 ± 2.2	134.8 ± 11.6[b]	174.2 ± 41.1	436.7 ± 36.8[d,f]
Terminal plasma AST (U/L)	139.0 ± 28.2	213.8 ± 31.6	338.9 ± 87.7	552.6 ± 49.5[c,f]
Baseline plasma TC (mmol/L)	2.1 ± 0.1	6.8 ± 0.3[b]	3.5 ± 0.2	10.4 ± 0.9[d,f]
Terminal plasma TC (mmol/L)	2.3 ± 0.1	6.7 ± 0.4[b]	4.4 ± 0.2	10.8 ± 0.6[d,f]
Baseline plasma TG (mmol/L)	0.7 ± 0.1	0.9 ± 0.1	1.1 ± 0.2	0.8 ± 0.1
Terminal plasma TG (mmol/L)	0.8 ± 0.1	1.0 ± 0.1	1.3 ± 0.1	0.7 ± 0.1[d]
OGTT-AUC	1104 ± 49.7	1217 ± 39.9	1612 ± 173.4	1319 ± 61.4
Fasting blood glucose (mmol/L)	7.3 ± 0.3	7.6 ± 0.2	8.1 ± 0.3	7.6 ± 0.3
Plasma insulin (pmol/L)	30.6 ± 6.7	97.4 ± 18.3	1189 ± 94	567.3 ± 123[d,e]
Baseline steatosis score (0-3)	0	2.7 ± 0.3[b]	1.8 ± 0.2	2.7 ± 0.3
Baseline fibrosis stage (0-4)	0	1.8 ± 0.2	0.25 ± 0.2	2.7 ± 0.3[d,f]
Terminal NAFLD activity score (0-8)	0	4.7 ± 0.4[b]	2.4 ± 0.3	6.3 ± 0.2[d]
Terminal steatosis score (0-3)	0	2.8 ± 0.1[b]	2.1 ± 0.2	2.1 ± 0.2
Terminal inflammation score (0-3)	0	1.4 ± 0.2[b]	0.3 ± 0.2	2.4 ± 0.2[d]
Terminal ballooning degeneration score (0-2)	0	0.4 ± 0.1	0	0.9 ± 0.1[d]
Terminal fibrosis stage (0-4)	0	1.2 ± 0.2[a]	0.1 ± 0.1	3.0 ± 0.2[d,e]
Terminal steatosis (% area)	5.4 ± 0.5	33.9 ± 2.6[b]	29.5 ± 2.3	41.2 ± 1.0[c]
Terminal fibrosis (% area)	0.3 ± 0.1	1.1 ± 0.2	1.2 ± 0.2	4.9 ± 0.7[d,e]
Terminal BW (g)	28.0 ± 0.3	39.1 ± 1.1	59 ± 1.1	54.8 ± 0.8[e]
Terminal lean tissue mass (g)	14.6 ± 0.8	18.8 ± 0.5[b]	19.9 ± 0.9	17.3 ± 0.4[c]
Terminal lean tissue mass (% of BW)	49.6 ± 2.6	47.7 ± 1.5	33.6 ± 1.1	31.9 ± 0.6[f]
Terminal fat tissue mass (g)	1.5 ± 0.1	8.1 ± 0.7[b]	25.1 ± 0.7	22.5 ± 0.5[c,f]
Terminal fat tissue mass (% of BW)	5.1 ± 0.5	20.0 ± 1.3[b]	42.3 ± 0.8	41.5 ± 0.5[f]
Liver weight (g)	1.1 ± 0.1	2.5 ± 0.3[b]	2.9 ± 0.2	5.4 ± 0.2[d,f]
Liver weight (% of BW)	3.9 ± 0.3	6.3 ± 0.6[b]	4.9 ± 0.3	9.9 ± 0.3[d,f]

[a]$P < 0.05$ *vs* lean chow, [b]$P < 0.01$ *vs* lean chow, [c]$P < 0.05$ *vs ob/ob* chow, [d]$P < 0.01$ *vs ob/ob* chow, [e]$P < 0.05$ *vs* DIO-NASH and [f]$P < 0.01$ *vs* DIO-NASH. NASH: Nonalcoholic steatohepatitis; ALT: Alanine aminotransferase; AST: Aspartate aminotransferase; BW: Body weight; OGTT: Oral glucose tolerance test; AUC: Area under the curve.

indicating that the NASH diet markedly alters the overall gene expression profile (Figure 2A). We identified a total of 1378 differentially expressed genes, composed of 510 repressed and 868 induced genes (Figure 2B). To explore biological processes affected, sets of significantly altered signaling pathways were extracted (Figure 2C and D). Many of these pathways are consistent with the observed NASH phenotype including focal adhesion, toll-like receptor (TLR) signaling pathway, matrix metalloproteinases and inflammatory response pathway. Consistent with the identification of focal adhesion as the top affected pathways multiple collagen subtypes showed increased expression (Figure 2E).

Similar analyses were conducted on a subset of samples from *ob*/*ob*-NASH animals which confirmed the exaggerated expression levels of collagen types (Figure 2E). The pathway analysis also highlighted TLR signaling as one of the primary affected signaling processes, an observation supported by the increased expression of TLR4, which was recently demonstrated as an important pro-inflammatory mediator in the pathogenesis of NASH[22,23]. Notably, mRNA expression levels of a number of other TLR subtypes (TLR7, TLR8, TLR12 and TLR13) were upregulated to greater extent than TLR4 (Figure 2F). Furthermore, a large collection of pro-inflammatory factors ranging from chemokines, such as monocyte chemoattractant protein-1 (MCP-1), to chemokine receptors, such as C-C motif chemokine receptor-2 (Ccr2) and macrophage markers (*i.e.*, CD68, CD86, F4-80 and MAC-2) (Figure 2G) were significantly induced. Finally, in line with observed hepatosteatosis, expression levels of genes involved in triglyceride biosynthesis were significantly increased in C57 and ob/ob animals exposed to the AMLN diet. Conversely, cholesterol biosynthesis expression was significantly decreased in the DIO-NASH and *ob*/*ob*-NASH mice (Figure 2H).

Male C57 and ob/ob mice sustained adiposity and elevated plasma metabolic parameters after AMLN diet-maintenance and repeated dosing intervention period

During the intervention period with diet-maintenance and repeated vehicle dosing for a total of 8 wk, DIO-NASH mice progressively gained body weight (adiposity), when compared to lean chow animals. Leptin-deficient mice also gained fat mass during the 8-wk intervention period (Figure 1E and F). Fat gain was somewhat less in the *ob*/*ob*-NASH mice, however, these mice began the study with a higher % adiposity (37%, *n* = 10) relative to DIO-NASH mice (14%, *n* = 12). At study end (termination), DIO-NASH and *ob*/*ob*-NASH animals sustained the elevated levels of plasma liver enzymes and hypercholesterolemia, when compared to respective chow-fed mice (Table 1). In contrast, terminal plasma TG levels were unchanged in DIO-NASH mice, and were significantly decreased for *ob*/*ob*-NASH animals,

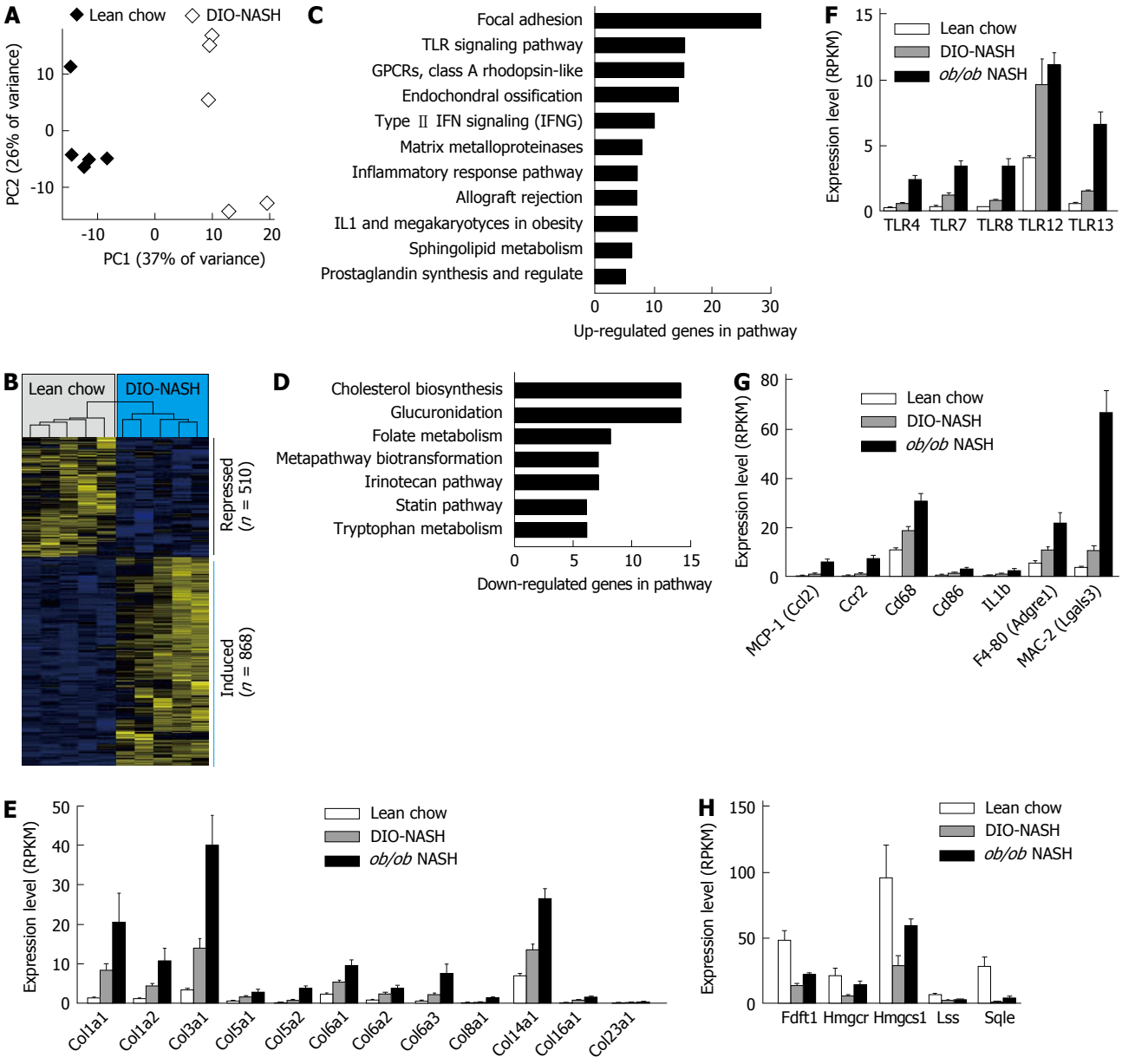

Figure 2 Gene expression analysis by RNAsequencing and bioinformatics. A: Principal component analysis of the 500 most variable genes, [principal component (PC)]; B: Hierarchical clustering of the differentially expressed genes, bars on the right indicate the induced and repressed genes; C: Pathways enriched for the induced (up-regulated) genes, filtered for $P < 0.01$ and $n > 4$; D: Same as (C) for the down-regulated genes; E-H: Expression levels of selected differentially expressed genes shown as mean ± SEM. Lean chow ($n = 5$), DIO-NASH ($n = 5$), *ob/ob* NASH ($n = 5$). NASH: Nonalcoholic steatohepatitis; BW: Body weight; TLR: Toll-like receptor; IFN: Interferon; IL1: Interleukine 1; MCP-1: Monocyte chemoattractant protein-1; GPCRs: G protein-coupled receptors; IFNG: Interferon gamma; RPKM: Reads per kilobase of transcript per million mapped reads; SEM: Standard error of the mean.

when compared to chow (Table 1). Collectively, terminal plasma levels of ALT, AST and TC were markedly elevated in *ob*/*ob*-NASH, when compared to DIO-NASH mice (Table 1).

An OGTT was performed four weeks into the intervention period. Fasting blood glucose and OGTT AUC for blood glucose were unchanged in DIO-NASH and *ob*/*ob*-NASH mice, as compared to respective chow fed animals (Table 1). Diet effects on glycemic status are supported by the elevation in plasma insulin levels of about 3-fold (NS) in DIO-NASH when compared to lean chow, whereas *ob*/*ob*-NASH showed a surprisingly decrease in plasma insulin levels at study end when compared to *ob*/*ob* chow animals (Table 1).

Male C57 and ob/ob mice demonstrated hepatomegaly with increased hepatic lipids and collagen content after AMLN diet-maintenance and repeated dosing intervention period

At study end, terminal liver weight was significantly increased in DIO-NASH and *ob*/*ob*-NASH mice, when compared to respective chow animals (Figure 3A). Additionally, liver weight of *ob*/*ob*-NASH was significantly higher than liver weight of DIO-NASH animals (Figure 3A). Both strains demonstrated increased deposition of liver TG and TC when compared to respective chow mice

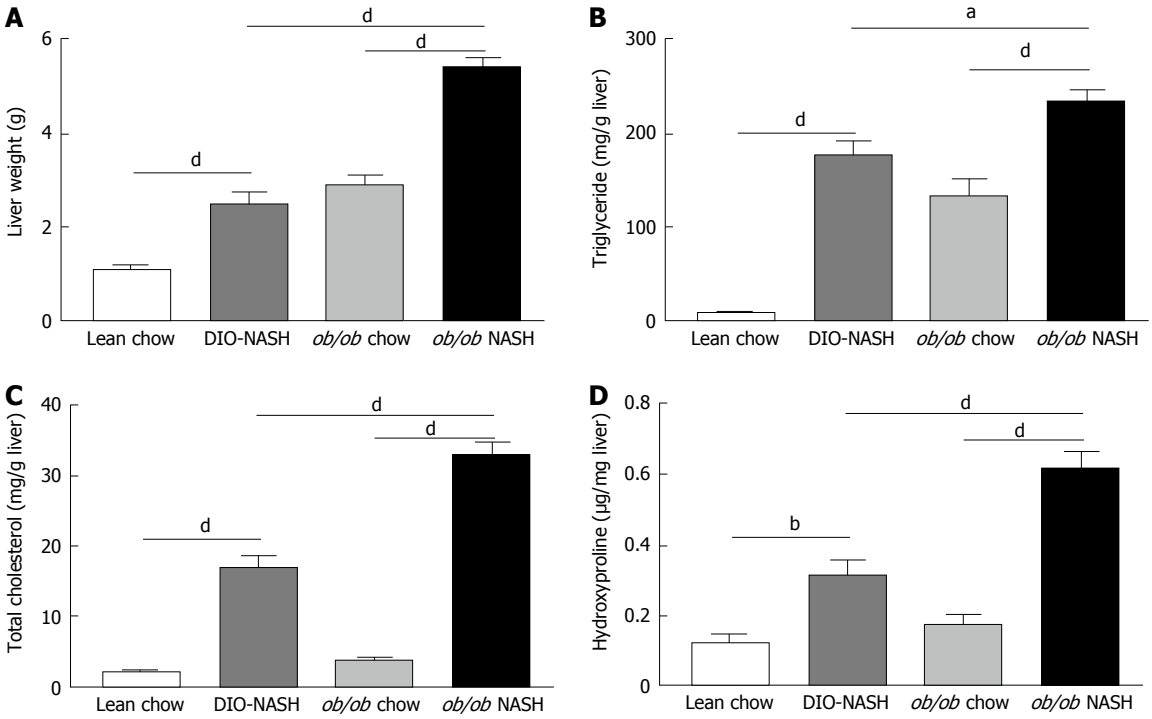

Figure 3 Liver weight and hepatic lipid and collagen content at study end. Liver weight at termination (A), hepatic triglyceride content (B), hepatic total cholesterol content (C), and hepatic hydroxyproline (collagen) content (D) at study end. $^{a}P < 0.05$, $^{b}P < 0.01$, $^{d}P < 0.001$. The results are presented as mean ± SEM. Lean chow (n = 9), DIO-NASH (n = 12), *ob/ob* chow (n = 8), *ob/ob* NASH (n = 10). NASH: Nonalcoholic steatohepatitis; BW: Body weight; SEM: Standard error of the mean.

(Figure 3B and C). Furthermore, liver TG and TC content were significantly increased in *ob*/*ob*-NASH mice, when compared to DIO-NASH animals (Figure 3B and C). Notably, DIO-NASH and *ob*/*ob*-NASH mice showed elevated levels of liver hydroxyproline (collagen) content, when compared to chow controls (Figure 3D). Overall, levels of liver hydroxyproline content were higher in *ob*/*ob*-NASH animals relative to DIO-NASH mice (Figure 3D).

Histopathological scoring of liver steatosis, inflammation and ballooning degeneration after AMLN diet-maintenance and repeated dosing intervention period in male C57 and ob/ob mice

Blinded histological assessment of NAS was performed on hematoxylin and eosin stained terminal hepatic tissue (Table 1). No evidence of steatosis, inflammation and ballooning degeneration was observed in lean chow controls (Figure 4A). In *ob*/*ob* chow mice steatosis was categorized as pronounced microvesicular with mild microvesicular steatosis (Figure 4B). Despite increased steatosis when maintained on chow diet, neither ballooning degeneration nor inflammation was observed in *ob*/*ob* chow animals (Figure 4B). In contrast, DIO-NASH mice developed micro- and macro-vesicular steatosis, with inflammation and ballooning degeneration (Figure 4C). Similarly, *ob*/*ob*-NASH mice developed micro- and macro-vesicular steatosis, and more pronounced inflammation and ballooning degeneration (Figure 4D). Thus, the NASH phenotypes of both strains of mice were clearly reflected in significantly increased NAS, when compared to respective chow animals (Figure 4E). Finally, image analysis confirmed hepatic steatosis in DIO-NASH and *ob*/*ob*-NASH mice (Figure 4F).

Histopathological scoring of liver fibrosis after AMLN diet-maintenance and repeated dosing intervention period in male C57 and ob/ob mice

Fibrosis stage was assessed by blinded histological evaluation using Sirius red staining of terminal liver tissue (Table 1). Hepatic fibrosis was not observed in lean chow or *ob*/*ob* chow mice (Figure 5A and B). In contrast, fibrosis was observed in DIO-NASH mice (Figure 5C) and to a greater extent in *ob*/*ob*-NASH animals who progressed to bridging fibrosis (Figure 5D). Fibrosis was most evident at tissue margins, but also penetrated into the tissue (Figure 5A-D). The fibrotic phenotypes of the DIO-NASH and *ob*/*ob*-NASH mice were mirrored by an increase in fibrosis stage compared to respective chow animals (Figure 5E). Increases in fibrosis stage were reflected by our image analyses showing an increase in % fractional area of Sirius Red (Figure 5F). Notably, the *ob*/*ob*-NASH animals were more fibrotic than DIO-NASH mice (Figure 5E and F).

DISCUSSION

In the present study two obese mouse models of diet-induced NASH were evaluated; the C57 DIO-NASH and the *ob*/*ob*-NASH. We confirm that a diet high in trans-fat, fructose and cholesterol produces a metabolic NASH phenotype with elevated plasma liver enzymes,

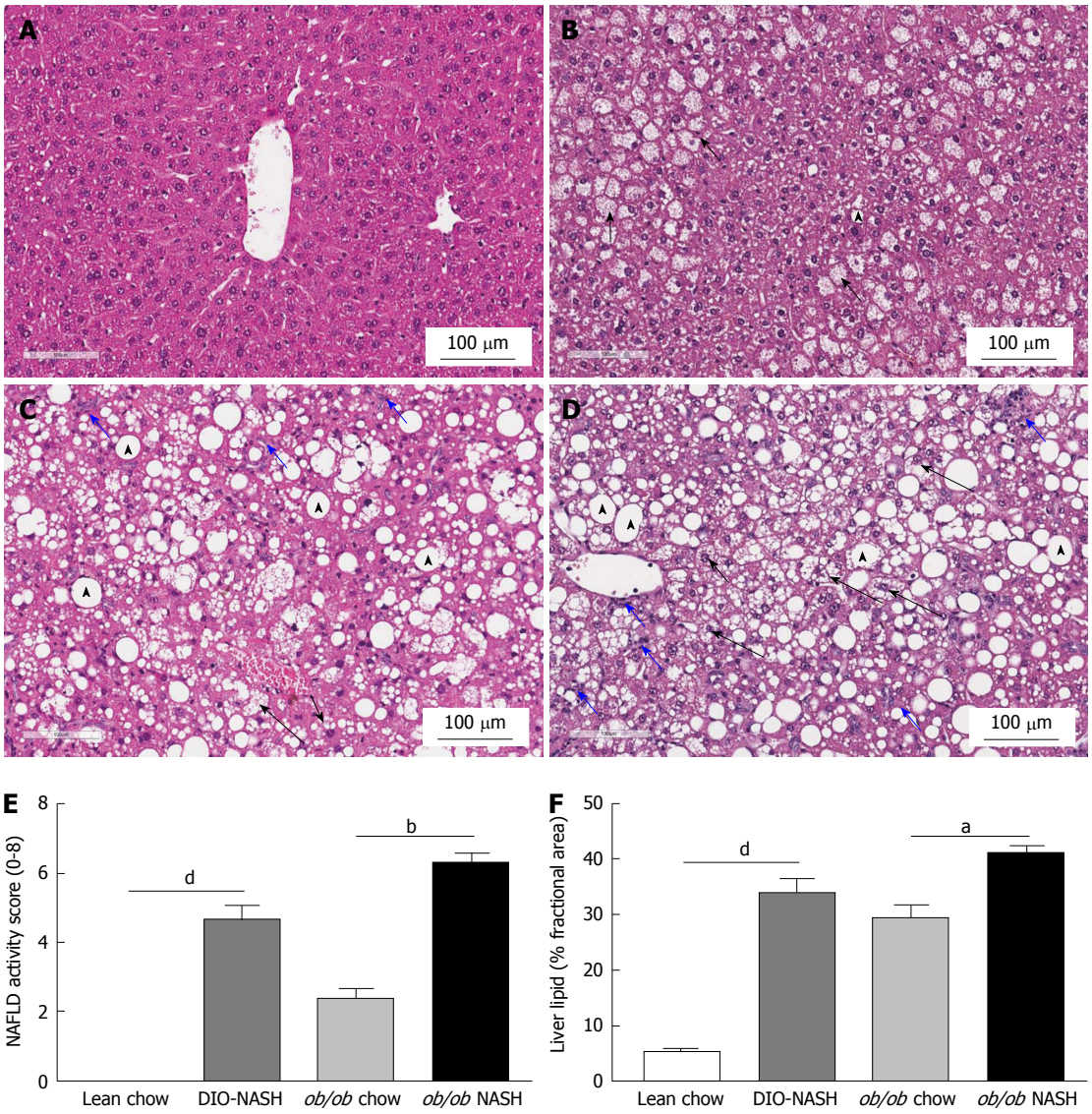

Figure 4 Histological assessment of non-alcoholic fatty liver disease activity score and liver lipid at study end. Representative H and E stained sections from; lean chow (A), *ob/ob* chow (B), DIO-NASH (C) and *ob/ob* NASH (D) mouse models. NAFLD activity score (steatosis, inflammation and ballooning degeneration) performed by a blinded pathologist at study end (E), and quantitatively image analysis of steatosis (% area) from H and E staining using visiomorph software (F). Macrovesicular steatosis indicated by arrowheads, microvesicular steatosis indicated by short black arrows, inflammation indicated by short blue arrows, ballooning degeneration indicated by long black arrows. $^{a}P < 0.05$, $^{b}P < 0.01$, $^{d}P < 0.001$. The results are presented as mean ± SEM. Lean chow (n = 9), DIO-NASH (n = 12), *ob/ob* chow (n = 8), *ob/ob* NASH (n = 10). NASH: Nonalcoholic steatohepatitis; NAFLD: Nonalcoholic fatty liver disease; SEM: Standard error of the mean.

hepatomegaly and recapitulates multiple clinical features including key hallmarks of NASH (steatosis, inflammation, ballooning degeneration and fibrosis). These changes were associated with marked alterations in associated gene expression pathways implicated in NASH and development of fibrosis. The mouse models are also suitable for pharmacological intervention studies, with a paired baseline liver biopsy procedure enabling individual disease stage before a repeated dosing period as is customary in NASH preclinical studies. Whereas all mice experienced slight weight loss following the biopsy, they returned to a weight stable state within one week moreover DIO-NASH and *ob/ob*-NASH sustained hepatomegaly, hepatic steatosis, inflammation, ballooning degeneration and fibrosis following repeated dosing intervention for a total of 8 wk.

DIO-NASH and *ob/ob*-NASH mice developed key hallmarks of fibrotic NASH including marked hepatosteatosis with evident inflammation and ballooning degeneration, as assessed by a clinical-derived histological NAS and fibrosis stage classification system developed by Kleiner *et al*[20]. This is in line with recent findings by Clapper *et al*[6] and Honda *et al*[24] in C57 AMLN mice, thus supporting the wild-type C57 DIO-NASH mouse as a suitable preclinical model for diet-induced obesity and NASH. In addition, the genetically obese ob/ob mouse model was also recently demonstrated to exhibit fibrotic NASH when fed AMLN diet[11,25]. In the leptin-deficient model superimposing the NASH diet high in trans-fat, fructose and cholesterol represents a "second hit" in development of preclinical NASH. The present study demonstrates that the NAS

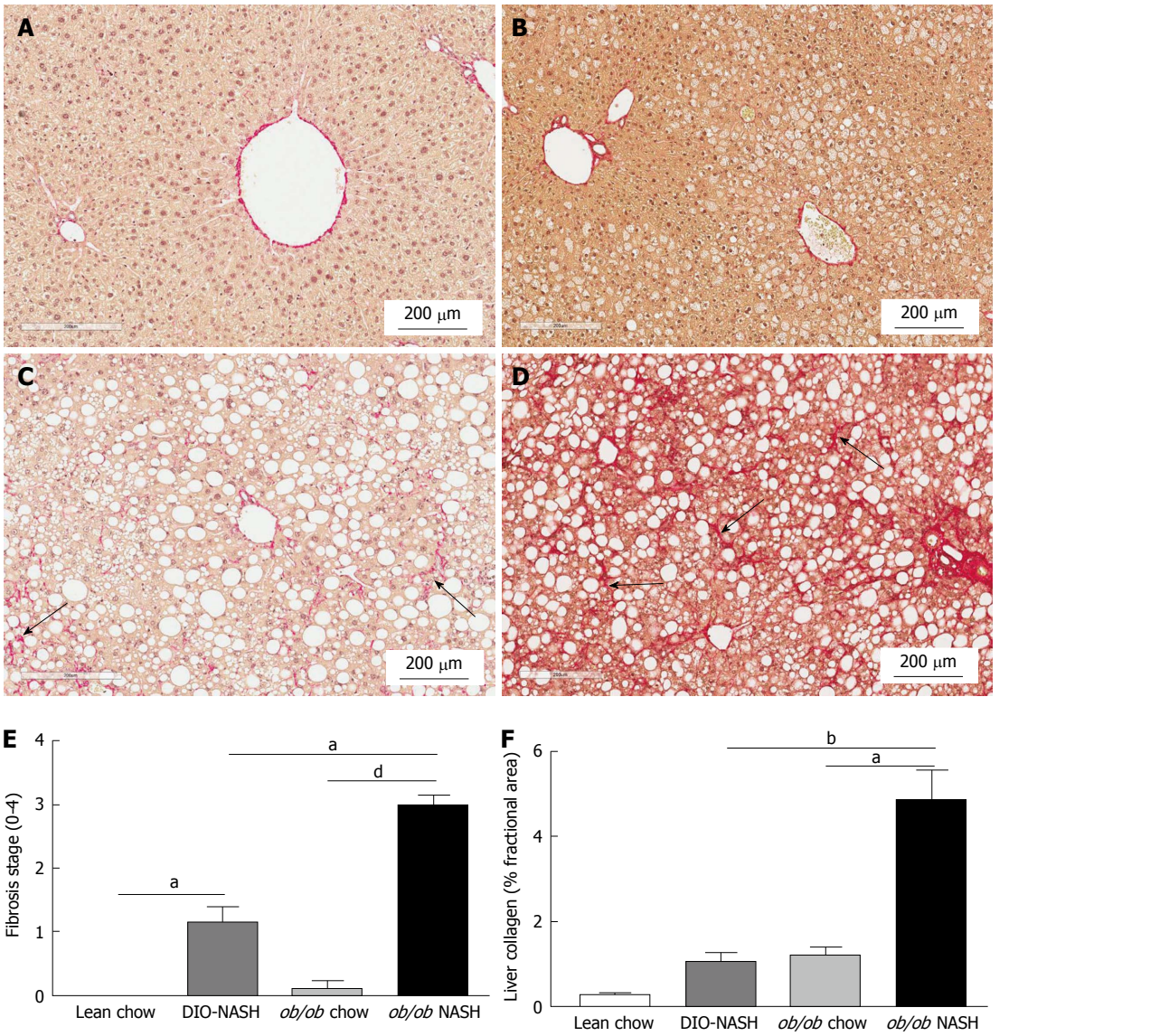

Figure 5 Histological assessment of fibrosis stage and liver collagen at study end. Representative sirius red stained sections from; lean chow (A), *ob/ob* chow (B), DIO-NASH (C) and *ob/ob* NASH (D) mouse model. Liver fibrosis stage performed by a blinded pathologist at study end (E), and quantitatively image analysis of collagen (% area) from sirius red staining using visiomorph software (F). Fibrous band formation indicated by black arrows. $^{a}P < 0.05$, $^{b}P < 0.01$, $^{d}P < 0.001$. The results are presented as mean ± SEM. Lean chow (n = 9), DIO-NASH (n = 12), *ob/ob* chow (n = 8), *ob/ob* NASH (n = 10). NASH: Nonalcoholic steatohepatitis; SEM: Standard error of the mean.

and fibrosis stage can also be integrated in analyses of the *ob*/*ob*-NASH mouse - and in conjunction with the excessive accumulation of hepatic lipids and collagen content - introduces an accelerated and aggressive diet-induced NASH phenotype relative to the C57 DIO-NASH model.

In accordance with histological observations of hepatic inflammation, mRNA analyses revealed within inflammatory pathways that toll-like receptors and downstream pro-inflammatory effectors (*e.g.,* Il1b, MCP-1) were markedly upregulated after the diet-induction period in DIO-NASH and *ob*/*ob*-NASH. In line with previous findings in diet-induced NASH mouse models[26], we observed increased expression of TLR4, a key receptor in fibrogenic development as demonstrated in high-fat diet-induced TLR4 knockout[22], and bile duct ligation models[23]. In addition, TLR4 KO in *ob*/*ob* mice was protective against NASH development as evinced by reduced NAS compared to regular *ob*/*ob* mice[27]. Interestingly, we observed higher expression levels of four additional TLRs: TLR7, TLR8, TLR12 and TLR13, which could be of relevance in future elucidation of the pathogenesis of NASH and for pharmacological intervention.

CCR2 mRNA levels were also increased in *ob*/*ob*-NASH mice. CCR2 has been implicated in the development of liver fibrosis, with $Ccr2^{-/-}$ mice showing reduced fibrosis following bile duct ligation or CCl_4 exposure[28]. CCR2 is a functional receptor for MCP-1, and is involved in the migration of macrophages during obesity[29]. Together, the impact on TLR signaling and macrophage abundance indicates an accelerated inflammatory NASH

phenotype in the *ob*/*ob*-genotype. Furthermore, markers of macrophage infiltration CD68 and F4-80, were up-regulated in DIO-NASH and to a larger extent in *ob*/*ob*-NASH mice, hereby corroborating the histological finding of increased inflammation in the two models.

In accordance with histological observations of hepatic fibrosis, our mRNA analyses also revealed increased expression of fibrillary collagens. Of particular interest is the increased diet- and strain-induced regulation of type Ⅰ, Ⅲ and type Ⅳ collagen, as these are known to be abundantly increased in liver fibrosis[30,31]. Interestingly, we also report altered expression of type Ⅰ collagen α1 and α2 chain, type Ⅲ collagen α1, as well as type XIV collagen α1, which could be of relevance in development/progression from NASH to fibrosis and future design of anti-fibrotic agents.

Pathway analyses also shed light on the transcriptional regulation of the main enzymes involved in triglyceride and cholesterol biosynthesis induced by the AMLN diet in DIO-NASH and *ob*/*ob*-NASH mice. Expression of these enzymes are all regulated by SREBP transcription factors, with SREBP1 regulating triglyceride synthesis and SREBP2 regulating cholesterol synthesis[32]. We report significantly increased levels of total cholesterol in plasma and livers of DIO-NASH and *ob*/*ob*-NASH mice compared to respective chow groups. Interestingly, the gene markers for biosynthesis of cholesterol in the liver appear to be dramatically reduced for DIO-NASH and *ob*/*ob*-NASH, presumably to compensate for the intake of high level of cholesterol in the diet. However, to our surprise the same was not observed for the triglyceride synthesis as the main lipid enzymes showed increased expression (data not shown), albeit plasma levels of triglycerides were significantly decreased for *ob*/*ob*-NASH mice compared to *ob*/*ob* chow. This could be caused by impairment in VLDL secretion from the liver[6], as relative triglyceride content in the liver was significantly increased in livers of *ob*/*ob*-NASH compared to levels in livers from *ob*/*ob* chow. Dysfunctional VLDL synthesis and secretion has been suggested to be a key factor in the progression of simple steatosis to NASH[33]. The mechanism(s) of action involved in the perturbed lipid metabolism awaits further investigations.

In conclusion, the diet-induced DIO-NASH and *ob*/*ob*-NASH mouse models demonstrate metabolic and histological key hallmarks of NASH. A clinically-derived histopathological scoring system can be applied in the DIO-NASH and *ob*/*ob*-NASH mouse models, thereby introducing a preclinical platform for evaluation of novel NASH therapeutics. Finally, a liver biopsy procedure at baseline allows for evaluation of individual disease staging prior to pharmacological intervention hereby reducing biological variability.

COMMENTS

Background

Nonalcoholic steatohepatitis (NASH) is an emerging liver disease with increasing prevalence. There are currently no pharmacological agents specifically approved for the treatment of NASH and disease management is consequently focused on the correction of underlying risk factors such as obesity, insulin resistance and dyslipidemia.

Research frontiers

The lack of approved therapeutics has to some degree been attributed to the failure of animal models to faithfully represent the clinical condition (*e.g.*, disease progression and metabolic background) and the way NASH is assessed clinically (paired biopsies and validated histological methods). Hence, novel diet-induced NASH models that develop the appropriate metabolic phenotype with improved liver sampling methods are highly desirable as a preclinical platform for exploring novel NASH treatments.

Innovations and breakthroughs

The authors describe and characterize a wild-type C57 and a genetically (*ob*/*ob*) obese diet-induced mouse model of NASH and confirm previous findings demonstrating key hallmarks of metabolic deregulation and fibrotic NASH using biochemical, histological and gene expression endpoints. Notably, a liver biopsy-confirmed and clinically-derived histological NASH scoring and fibrosis staging are being performed in *ob*/*ob* mice, which the authors are the first to report. Finally, the utility of the diet-induced NASH mouse models for pharmacological investigations is being demonstrated by performing a chronic intervention period with repeated dosing following a baseline liver biopsy procedure.

Applications

A baseline liver biopsy performed after diet-induction allows for individual disease staging for stratification and randomization into study groups and for evaluation of novel NASH therapeutics.

Peer-review

The results of this study demonstrated a useful animal model for evaluation the disease progression and treatment of NASH. The data were appropriately presented and interpreted. The manuscript was well prepared.

REFERENCES

1 **Ariz U**, Mato JM, Lu SC, Martínez Chantar ML. Nonalcoholic steatohepatitis, animal models, and biomarkers: what is new? *Methods Mol Biol* 2010; **593**: 109-136 [PMID: 19957147 DOI: 10.1007/978-1-60327-194-3]

2 **Adams LA**, Sanderson S, Lindor KD, Angulo P. The histological course of nonalcoholic fatty liver disease: a longitudinal study of 103 patients with sequential liver biopsies. *J Hepatol* 2005; **42**: 132-138 [PMID: 15629518 DOI: 10.1016/j.jhep.2004.09.012]

3 **Zeevaart JG**, Wang L, Thakur VV, Leung CS, Tirado-Rives J, Bailey CM, Domaoal RA, Anderson KS, Jorgensen WL. Optimization of azoles as anti-human immunodeficiency virus agents guided by free-energy calculations. *J Am Chem Soc* 2008; **130**: 9492-9499 [PMID: 18588301 DOI: 10.1021/ja8019214]

4 **Farrell GC**, Larter CZ. Nonalcoholic fatty liver disease: from steatosis to cirrhosis. *Hepatology* 2006; **43**: S99-S112 [PMID: 16447287 DOI: 10.1002/hep.20973]

5 **Day CP**, James OF. Steatohepatitis: a tale of two "hits"? *Gastroenterology* 1998; **114**: 842-845 [PMID: 9547102 DOI: 10.1016/S0016-5085(98)70599-2]

6 **Clapper JR**, Hendricks MD, Gu G, Wittmer C, Dolman CS, Herich J, Athanacio J, Villescaz C, Ghosh SS, Heilig JS, Lowe C, Roth JD. Diet-induced mouse model of fatty liver disease and nonalcoholic steatohepatitis reflecting clinical disease progression and methods of assessment. *Am J Physiol Gastrointest Liver Physiol* 2013; **305**: G483-G495 [PMID: 23886860 DOI: 10.1152/ajpgi.00079.2013]

7 **Sanches SC**, Ramalho LN, Augusto MJ, da Silva DM, Ramalho FS. Nonalcoholic Steatohepatitis: A Search for Factual Animal Models. *Biomed Res Int* 2015; **2015**: 574832 [PMID: 26064924 DOI: 10.1155/2015/574832]

8 **Machado MV**, Michelotti GA, Xie G, Almeida Pereira T, Boursier

J, Bohnic B, Guy CD, Diehl AM. Mouse models of diet-induced nonalcoholic steatohepatitis reproduce the heterogeneity of the human disease. *PLoS One* 2015; **10**: e0127991 [PMID: 26017539 DOI: 10.1371/journal.pone.0127991]

9 **Takahashi Y**, Soejima Y, Fukusato T. Animal models of nonalcoholic fatty liver disease/nonalcoholic steatohepatitis. *World J Gastroenterol* 2012; **18**: 2300-2308 [PMID: 22654421 DOI: 10.3748/wjg.v18.i19.2300]

10 **Starkel P**, Leclercq IA. Animal models for the study of hepatic fibrosis. *Best Pract Res Clin Gastroenterol* 2011; **25**: 319-333 [PMID: 21497748 DOI: 10.1016/j.bpg.2011.02.004]

11 **Trevaskis JL**, Griffin PS, Wittmer C, Neuschwander-Tetri BA, Brunt EM, Dolman CS, Erickson MR, Napora J, Parkes DG, Roth JD. Glucagon-like peptide-1 receptor agonism improves metabolic, biochemical, and histopathological indices of nonalcoholic steatohepatitis in mice. *Am J Physiol Gastrointest Liver Physiol* 2012; **302**: G762-G772 [PMID: 22268099 DOI: 10.1152/ajpgi.00476.2011]

12 **Tetri LH**, Basaranoglu M, Brunt EM, Yerian LM, Neuschwander-Tetri BA. Severe NAFLD with hepatic necroinflammatory changes in mice fed trans fats and a high-fructose corn syrup equivalent. *Am J Physiol Gastrointest Liver Physiol* 2008; **295**: G987-G995 [PMID: 18772365 DOI: 10.1152/ajpgi.90272.2008]

13 **Nakayama H**, Otabe S, Ueno T, Hirota N, Yuan X, Fukutani T, Hashinaga T, Wada N, Yamada K. Transgenic mice expressing nuclear sterol regulatory element-binding protein 1c in adipose tissue exhibit liver histology similar to nonalcoholic steatohepatitis. *Metabolism* 2007; **56**: 470-475 [PMID: 17379003 DOI: 10.1016/j.metabol.2006.11.004]

14 **Chen H**, Charlat O, Tartaglia LA, Woolf EA, Weng X, Ellis SJ, Lakey ND, Culpepper J, Moore KJ, Breitbart RE, Duyk GM, Tepper RI, Morgenstern JP. Evidence that the diabetes gene encodes the leptin receptor: identification of a mutation in the leptin receptor gene in db/db mice. *Cell* 1996; **84**: 491-495 [PMID: 8608603 DOI: 10.1016/S0092-8674(00)81294-5]

15 **Dobin A**, Davis CA, Schlesinger F, Drenkow J, Zaleski C, Jha S, Batut P, Chaisson M, Gingeras TR. STAR: ultrafast universal RNA-seq aligner. *Bioinformatics* 2013; **29**: 15-21 [PMID: 23104886 DOI: 10.1093/bioinformatics/bts635]

16 **Anders S**, Pyl PT, Huber W. HTSeq--a Python framework to work with high-throughput sequencing data. *Bioinformatics* 2015; **31**: 166-169 [PMID: 25260700 DOI: 10.1101/002824]

17 **Robinson MD**, McCarthy DJ, Smyth GK. edgeR: a Bioconductor package for differential expression analysis of digital gene expression data. *Bioinformatics* 2010; **26**: 139-140 [PMID: 19910308 DOI: 10.1093/bioinformatics/btp616]

18 **Kutmon M**, Riutta A, Nunes N, Hanspers K, Willighagen EL, Bohler A, Mélius J, Waagmeester A, Sinha SR, Miller R, Coort SL, Cirillo E, Smeets B, Evelo CT, Pico AR. WikiPathways: capturing the full diversity of pathway knowledge. *Nucleic Acids Res* 2016; **44**: D488-D494 [PMID: 26481357 DOI: 10.1093/nar/gkv1024]

19 **Kutmon M**, van Iersel MP, Bohler A, Kelder T, Nunes N, Pico AR, Evelo CT. PathVisio 3: an extendable pathway analysis toolbox. *PLoS Comput Biol* 2015; **11**: e1004085 [PMID: 25706687 DOI: 10.1371/journal.pcbi.1004085]

20 **Kleiner DE**, Brunt EM, Van Natta M, Behling C, Contos MJ, Cummings OW, Ferrell LD, Liu YC, Torbenson MS, Unalp-Arida A, Yeh M, McCullough AJ, Sanyal AJ. Design and validation of a histological scoring system for nonalcoholic fatty liver disease. *Hepatology* 2005; **41**: 1313-1321 [PMID: 15915461 DOI: 10.1002/hep.20701]

21 **Wang Z**, Gerstein M, Snyder M. RNA-Seq: a revolutionary tool for transcriptomics. *Nat Rev Genet* 2009; **10**: 57-63 [PMID: 19015660 DOI: 10.1038/nrg2484]

22 **Sutter AG**, Palanisamy AP, Lench JH, Esckilsen S, Geng T, Lewin DN, Cowart LA, Chavin KD. Dietary Saturated Fat Promotes Development of Hepatic Inflammation Through Toll-Like Receptor 4 in Mice. *J Cell Biochem* 2016; **117**: 1613-1621 [PMID: 26600310 DOI: 10.1002/jcb.25453]

23 **Seki E**, De Minicis S, Osterreicher CH, Kluwe J, Osawa Y, Brenner DA, Schwabe RF. TLR4 enhances TGF-beta signaling and hepatic fibrosis. *Nat Med* 2007; **13**: 1324-1332 [PMID: 17952090 DOI: 10.1038/nm1663]

24 **Honda Y**, Imajo K, Kato T, Kessoku T, Ogawa Y, Tomeno W, Kato S, Mawatari H, Fujita K, Yoneda M, Saito S, Nakajima A. The Selective SGLT2 Inhibitor Ipragliflozin Has a Therapeutic Effect on Nonalcoholic Steatohepatitis in Mice. *PLoS One* 2016; **11**: e0146337 [PMID: 26731267 DOI: 10.1371/journal.pone.0146337]

25 **Griffett K**, Welch RD, Flaveny CA, Kolar GR, Neuschwander-Tetri BA, Burris TP. The LXR inverse agonist SR9238 suppresses fibrosis in a model of non-alcoholic steatohepatitis. *Mol Metab* 2015; **4**: 353-357 [PMID: 25830098 DOI: 10.1016/j.molmet.2015.01.009]

26 **Rivera CA**, Adegboyega P, van Rooijen N, Tagalicud A, Allman M, Wallace M. Toll-like receptor-4 signaling and Kupffer cells play pivotal roles in the pathogenesis of non-alcoholic steatohepatitis. *J Hepatol* 2007; **47**: 571-579 [PMID: 17644211 DOI: 10.1016/j.jhep.2007.04.019]

27 **Sutter AG**, Palanisamy AP, Lench JH, Jessmore AP, Chavin KD. Development of steatohepatitis in Ob/Ob mice is dependent on Toll-like receptor 4. *Ann Hepatol* 2015; **14**: 735-743 [PMID: 26256903]

28 **Seki E**, de Minicis S, Inokuchi S, Taura K, Miyai K, van Rooijen N, Schwabe RF, Brenner DA. CCR2 promotes hepatic fibrosis in mice. *Hepatology* 2009; **50**: 185-197 [PMID: 19441102 DOI: 10.1002/hep.22952.CCR2]

29 **Weisberg SP**, Hunter D, Huber R, Lemieux J, Slaymaker S, Vaddi K, Charo I, Leibel RL, Ferrante AW. CCR2 modulates inflammatory and metabolic effects of high-fat feeding. *J Clin Invest* 2006; **116**: 115-124 [PMID: 16341265 DOI: 10.1172/JCI24335]

30 **Bataller R**, Brenner DA. Liver fibrosis. *J Clin Invest* 2005; **115**: 209-218 [PMID: 15690074 DOI: 10.1172/JCI200524282]

31 **Friedman SL**. Mechanisms of hepatic fibrogenesis. *Gastroenterology* 2008; **134**: 1655-1669 [PMID: 18471545 DOI: 10.1053/j.gastro.2008.03.003]

32 **Horton JD**, Goldstein JL, Brown MS. SREBPs: activators of the complete program of cholesterol and fatty acid synthesis in the liver. *J Clin Invest* 2002; **109**: 1125-1131 [PMID: 11994399 DOI: 10.1172/JCI200215593]

33 **Fujita K**, Nozaki Y, Wada K, Yoneda M, Fujimoto Y, Fujitake M, Endo H, Takahashi H, Inamori M, Kobayashi N, Kirikoshi H, Kubota K, Saito S, Nakajima A. Dysfunctional very-low-density lipoprotein synthesis and release is a key factor in nonalcoholic steatohepatitis pathogenesis. *Hepatology* 2009; **50**: 772-780 [PMID: 19650159 DOI: 10.1002/hep.23094]

P- Reviewer: Chuang WL, Kim JS, Miura K **S- Editor**: Qi Y
L- Editor: A **E- Editor**: Liu SQ

Published by **Baishideng Publishing Group Inc**
8226 Regency Drive, Pleasanton, CA 94588, USA
Telephone: +1-925-223-8242
Fax: +1-925-223-8243
E-mail: bpgoffice@wjgnet.com
Help Desk: http://www.wjgnet.com/esps/helpdesk.aspx
http://www.wjgnet.com